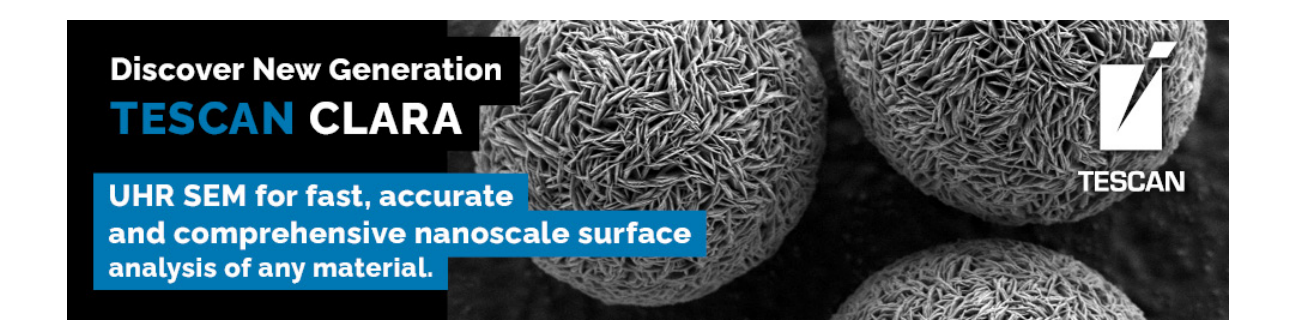
Pulse-Induced CDW Transitions in 1T-TaS2 Studied with in situ Cryo-TEM and Electric Biasing

James L Hart, Saif Siddique, Noah Schnitzer, Lena F Kourkoutis, Judy J Cha



Meeting-report

Microanalysis

Microscopy AND

Pulse-Induced CDW Transitions in 1T-TaS₂ Studied with in situ Cryo-TEM and Electric Biasing

James L Hart¹, Saif Siddique¹, Noah Schnitzer¹, Lena F Kourkoutis^{2,3}, and Judy J Cha¹

Quantum materials with coupled structural and electronic transitions are promising for next-generation computing devices. The engineering of such devices requires a detailed understanding of the phase transition pathways in nanoscale geometries. However, experimental insight into such processes is highly challenging. Here, we perform in situ cryogenic sample cooling and electric biasing within the (scanning) transmission electron microscope ((S)TEM) to reveal the structure-property coupling across a charge density wave (CDW) and insulator-to-metal transition (IMT) in a 2D quantum material.

We study the 2D transition metal dichalcogenide 1T-TaS₂, which undergoes a series of temperature driven CDW transitions, from the low-temperature commensurate (C) phase, to the intermediate temperature nearly commensurate (NC) phase, and then to the high temperature incommensurate (I) phase [1]. The low-temperature C-CDW phase is insulating, while the other CDW phases are metallic. The electronic resistivity can also be controlled by electric pulsing. Specifically, when a high electric field is applied to the insulating C-CDW phase, it undergoes a rapid transition to a metallic state [2]. This electrically-driven IMT has garnered great interest for 2-terminal devices, e.g., for neuromorphic computing. However, fundamental questions remain concerning this transition, such as how the IMT couples to the underlying CDW, and whether the transition is truly field-induced, or simply due to Joule heating. To address these questions, we track the CDW structure of 2-terminal TaS2 devices with in situ TEM cooling and electric biasing [3].

For these experiments we use a HennyZ double-tilt sample holder with continuously variable temperature ($\sim 100 - 1000 \, \mathrm{K}$) [4]. Fig. 1a shows an optical image of a TaS₂ device, and Fig. 1b shows the same device imaged within the STEM. The temperaturedependent resistance of the device is displayed in Fig. 1c, measured upon heating through the C-NC and NC-I phase transitions within the TEM. The IMT is clearly observed at ~ 230 K, concomitant with the C-NC CDW transition measured with selected area electron diffraction.

We next study in situ electric pulsing of the TaS₂ device in the C-phase at low temperature (~130 K). Our biasing set-up is shown in Fig. 2a, where a 3 μ s electric pulse is applied to the flake in series with a 1 μ 0 resistor. With this geometry, the voltage drop across the flake divided by the total applied voltage (V_{flake} / V_{total}) is proportional to the transient flake resistance. The pulse-induced IMT is observed for voltage pulses greater than ~ 3 V (Fig. 2b). To understand how the CDW evolves with pulsing, we continuously collected selected-area electron diffraction data using the electron microscope pixel array detector (EMPAD) with a 2 ms frame rate. Pre- and post-pulse diffraction patterns are shown in Fig. 2c for the 5.6 V pulse, which demonstrate a clear CDW transition. To quantify the CDW structure, we determine the position of all Bragg and CDW diffraction spots using a center-of-mass method. We can then track parameters such as the CDW angle, CDW wave vector, and lattice strain (Fig. 2d).

Our measurements show that the pulse-induced IMT is associated with a CDW transition from the C phase to the NC phase. Additionally, we find that the strength of the voltage pulse controls the rotation of the CDW pattern, which correlates with the relative change in electronic resistance. Based on the relative lattice strain after pulsing and the reported TaS₂ coefficient of thermal expansion [5], the degree of Joule heating appears insufficient to drive the C to NC phase transition. This finding suggests that the transition is field-induced, and not thermally induced. These findings are highly relevant to the engineering of 2-terminal TaS₂ electronic devices. Additionally, our study highlights the promise of in situ cryo-TEM and electric biasing for the study of quantum materials [6].

¹Department of Materials Science and Engineering, Cornell University, Ithaca, NY, USA

²School of Applied and Engineering Physics, Cornell University, Ithaca, NY, USA

³Kavli Institute at Cornell for Nanoscale Science, Cornell University, Ithaca, NY, USA

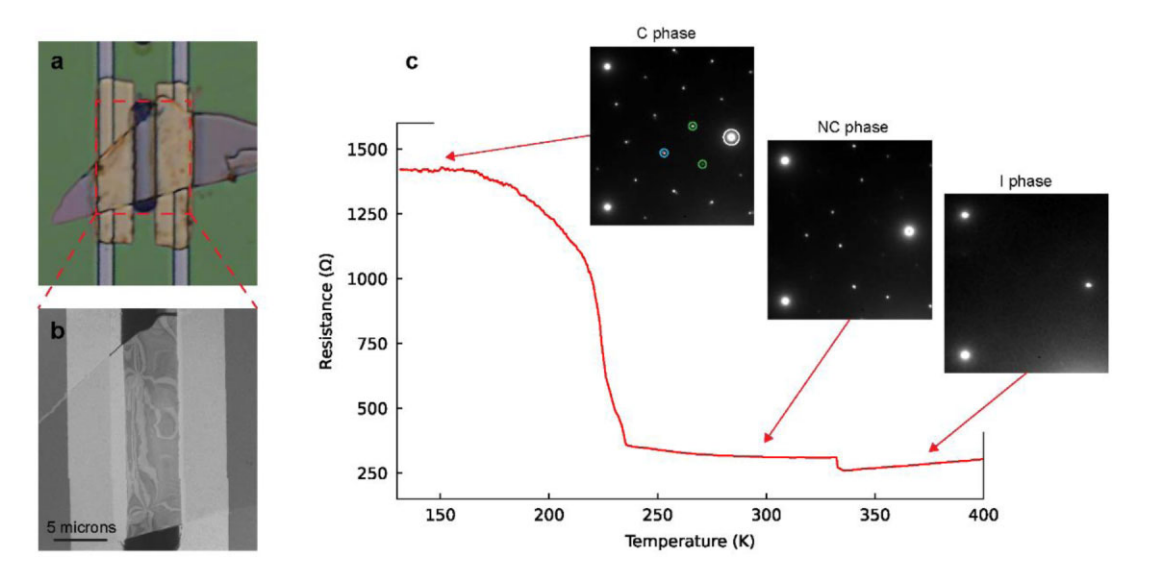


Fig. 1. a) Optical image of a TaS_2 device. The flake was transferred onto an *in situ* TEM chip with a PDMS stamp. The chip has pre-patterned Pt electrodes, and a through-hole for TEM viewing. We then deposited additional Cr / Au electrodes on top of the flake for improved electrical contact. **b)** STEM-ADF image of the same flake. **c)** *In situ* resistance versus temperature data for the device upon warming, with accompanying electron diffraction patterns. In the C phase diffraction pattern, the white circle marks a Bragg spot, the green circles mark 1^{st} order CDW spots, and the teal circle marks a 2^{nd} order CDW spot. Upon entering the NC phase, the intensity of the 1^{st} order CDW spots are greatly reduced, and the angle and length of the 2^{nd} order CDW spots are slightly altered.

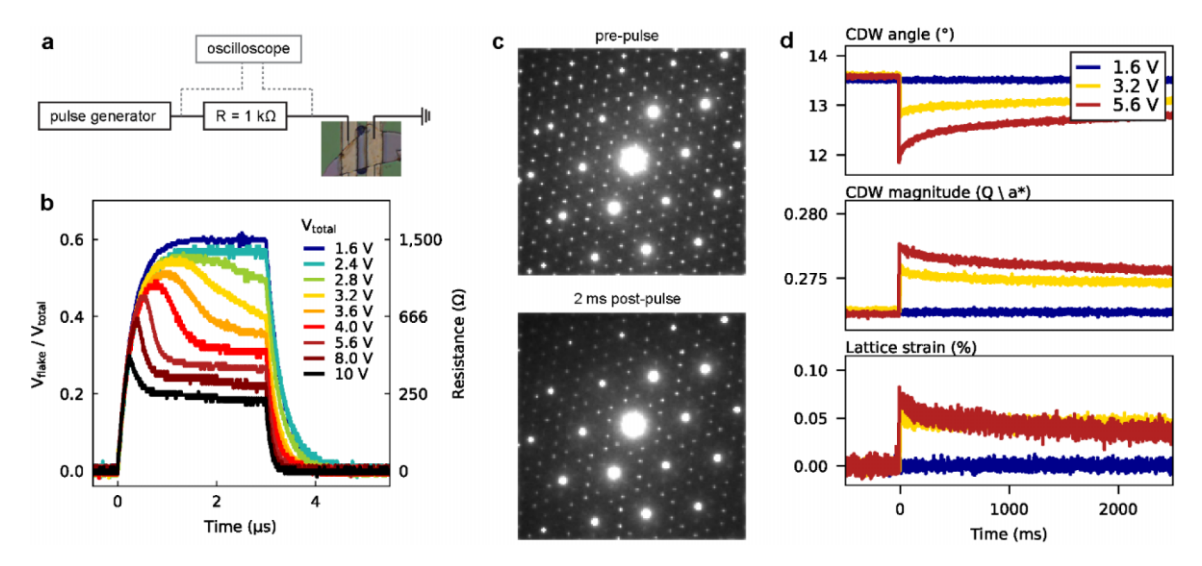


Fig. 2. a) Electrical set-up for *in situ* pulsing of the TaS₂ device. **b)** Voltage drop across the TaS₂ flake divided by the total applied voltage. The legend provides the applied voltage for each curve. **c)** Select TaS₂ diffraction data captured on the EMPAD during *in situ* electric pulsing. **d)** Analysis of the time-resolved EMPAD data showing the angle of the CDW lattice with respect to the underlying Bragg lattice (top), the magnitude of the CDW wavevector relative to the Bragg lattice (middle), and the measured in-plane lattice strain (bottom).

References

- 1. B Sipos et al, Nature Materials 7 (2008), p. 960.
- 2. I Vaskivskyi et al, Nature Communications 7 (2016), p. 11442.
- 3. J Hart and J Cha, Nanoletters 21 (2021), p. 5449.
- 4. B Goodge et al, Microscopy and Microanalysis 26 (2020), p. 439.
- 5. F Givens and G Fredericks, J. Phys. Chem. Solids 38 (1977), p. 1363.
- 6. JL Hart and JJ Cha were funded through the Gordon and Betty Moore foundation (EPiQS Synthesis Award). Device fabrication was performed in part at the Cornell NanoScale Facility, a member of the National Nanotechnology Coordinated Infrastructure (NNCI), which is supported by the National Science Foundation (Grant NNCI-2025233). This work made use of the electron microscopy facility of the Platform for the Accelerated Realization, Analysis, and Discovery of Interface Materials (PARADIM), which is supported by the National Science Foundation under Cooperative Agreement No. DMR-2039380, and the Cornell Center for Materials Research Shared Facilities which are supported through the NSF MRSEC program (DMR-1719875). The FEI Titan Themis 300 was acquired through NSF-MRI-1429155, with additional support from Cornell University, the Weill Institute and the Kavli Institute at Cornell.



TESCAN TENSOR

Integrated, Precession-Assisted, Analytical 4D-STEM





Visit us and learn more about our TESCAN TENSOR

info.tescan.com/stem